ACS OMEGA

Open Access

http://pubs.acs.org/journal/acsodf

Article

Simple Preparation and Bone Regeneration Effects of Poly(vinyl alcohol)−Resveratrol Self-Cross-Linked Hydrogels

Pengyin Li, Shaoqing Chen, Yanyan Meng, Cheli Wang,* and Xinye Ni*

Cite This: *ACS Omega* 2024, 9, 49043−49053

Read Online

ACCESS | Metrics & More | Article Recommendations | Supporting Information

ABSTRACT: Hydrogels have broad application prospects in bone repair. Pure poly(vinyl alcohol) (PVA) hydrogels have limited applications because of their low hardness and poor mechanical properties. This study found that resveratrol (Res) and PVA self-assembled and cross-linked through the formation of strong hydrogen bonds after freeze−thawing, forming an easily available PVA−Res supramolecular hydrogel through a green process. PVA−Res hydrogels with different Res wt %:10 wt % PVA ratios were prepared through freeze−thawing and designated as 0.4, 1.2, and 2.0 wt % PVA−Res hydrogels. Rheological studies demonstrated that the viscoelastic modulus of the PVA−Res hydrogels was significantly improved compared to pure PVA hydrogels. The viscoelastic modulus G' of 1.2% PVA−Res hydrogel was 2299 Pa, which was 8.5-fold that of the pure PVA hydrogel. We conducted a study on cell proliferation and osteogenic differentiation using MC3T3-E1 (preosteoblasts from newborn mouse calvaria). The results showed that the 0.4% PVA-Res hydrogel promotes alkaline phosphatase activity and mineral deposition. Real-time quantitative PCR (RT-qPCR) analysis demonstrated that the 0.4% PVA−Res hydrogel upregulated the expression of osteogenic differentiation-related genes (BMP-9, OCN, and ALP). Furthermore, RT-qPCR and flow cytometry demonstrated that the 0.4% PVA−Res hydrogel could effectively promote the M2 transformation and polarization of mouse mononuclear macrophage leukemia cells (Raw 264.7). The expression of related genes, such as Arg-1 and CD206, significantly increased, whereas that of M1 polarization-related genes, such as iNOS and TNF-α, significantly decreased. In summary, PVA−Res supramolecular hydrogels are potential materials for use in bone repair.

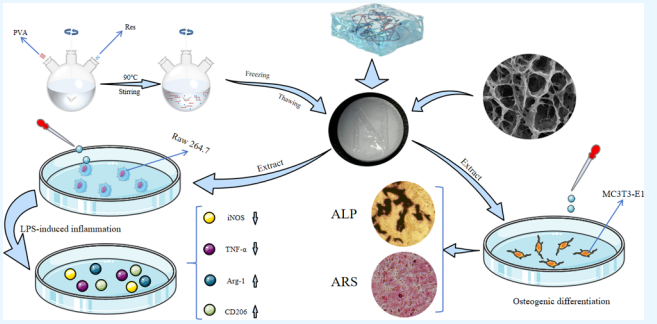

1. INTRODUCTION

Hydrogels polymerize into three-dimensional (3D) network structures and are widely used as biomaterials in drug carriers and biological scaffolds.[1] Given that hydrogels have nanoscale pore structures as well as favorable biocompatibility and controllability, they have become excellent candidate materials for bone tissue engineering.[2−4] Poly(vinyl alcohol) (PVA) is a polymer derived from the hydrolysis of polyvinyl acetate, known for its good biocompatibility, nontoxicity, hydrophilicity, and chemical stability. Additionally, it has the characteristic of being biodegradable when used as scaffold material.[5,6] The surface of PVA exhibits friction and tension resistance, and a state of high adhesion exists between its molecules. PVA-based hydrogels have been widely used in biomedical applications, such as drug-delivery systems, tissue engineering, and medical devices.[7−12] However, pure PVA solutions cannot spontaneously form hydrogels at 25 °C. Although PVA hydrogels formed by freeze−thaw crystallization can form semisolid hydrogels at 25 °C, their mechanical properties do not meet the requirements of normal gels, with an elastic modulus of 3717.0 MPa and an elongation at break of 11.9%.[13−15] The performance of most PVA-based hydrogels can be improved by adding other molecules, such as boric acid, borax, glutaraldehyde, and epichlorohydrin, to form strong covalent bonds or noncovalent cross-links between PVA chains. However, the toxicity of these agents limits the application of the resulting hydrogels.[16−19]

Natural compound molecules can self-assemble with PVA to form supramolecular hydrogels and effectively improve their mechanical properties.[20] Song et al. reported that luteolin can form strong hydrogen bonds with PVA to generate hydrogels. They provided a typical example of the cross-linking of representative hydrophobic flavonoids with PVA, and the results showed that only luteolin formed strong hydrogen bonds with PVA and that only 0.04 wt % luteolin was needed for cross-linking with PVA to form a hydrogel. The elongation rate and tensile strength of the resulting hydrogel reached 600% and 0.812 MPa, respectively, and were better than those

Received: March 25, 2024
Revised: November 14, 2024
Accepted: November 25, 2024
Published: December 3, 2024

of ordinary PVA water gel. Although the hydrogel had promising properties, its biologically relevant applications have not been proven.[21,22]

Resveratrol (Res) is a naturally occurring nonflavonoid polyphenolic compound. Res has attracted widespread attention in medicine and nutrition[23] and is believed to have multiple benefits and biological activities, including antioxidant, anti-inflammatory, antiaging, anticancer, cardiovascular protection, and immunomodulation effects.[24−26] Min et al. reported that osteogenic induction medium containing 25 μmol/L Res could increase the proliferation and alkaline phosphatase (ALP) activity of osteoblast-like cells (MC3T3-E1) derived from the calvaria of C57BL/6 mice, as well as enhance the expression of ALP, BMP-2, BMP-4, and cyanate-related genes. However, when the concentration of Res exceeded 25 μmol/L, the proliferation and ALP activity of MC3T3-E1 cells decreased.[27] Duan et al. reported that Res promoted macrophage autophagy by upregulating SIRT3 expression and AMP-activated protein kinase phosphorylation.[28] Yuan et al. showed that resveratrol exerted anti-inflammatory activity by activating the ERK1/2 pathway, decreasing the secretion of interleukin (IL)-6 and IL-8 induced by TNF-α, and enhancing human periodontal ligament stem cells osteogenesis.[29] However, like most other flavonoids, Res has poor water solubility due to its physical and chemical properties, which limits its further application in bone regeneration treatment.[30,31] The molecular structure of Res contains benzene rings and hydroxyl groups similar to those in curcumin and has a similar arrangement; therefore, if Res could be cross-linked with a PVA hydrogel in a similar manner to curcumin, this could become another potential natural cross-linking agent.

Herein, we found that Res is a potential cross-linking agent. The PVA−Res complex exhibited favorable stability and biological activity. Hydrogels were obtained through uniform mixing at 90 °C, followed by cooling to 25 °C. Given the crystallization of PVA and the presence of hydrogen bonds between PVA and Res, the PVA−Res hydrogels have greater stability and mechanical strength than ordinary PVA hydrogels. In addition, after freeze−thawing, the hydrogels exhibited specific biological effects and could induce bone repair and anti-inflammatory effects. We believe that our PVA−Res hydrogels represent a new type of green hydrogel biomaterial with a simple preparation process and are potential bone repair hydrogel materials.

2. MATERIALS AND METHODS

PVA (alcoholysis degree of 99%, M_w of 89,000−98,000) was purchased from Ron Reagent Co., Ltd. (Shanghai, China). Res ($C_{14}H_{12}O_3$, purity 99%) was purchased from Shanghai Aladdin Reagent Co., Ltd. (Shanghai, China). The mouse preosteoblastic cell line (MC3T3-E1) and mouse monocyte/macrophage leukemia cell line (Raw 264.7) were purchased from Creative Bioarray (Shanghai, China). MEM Alpha basic (1×), DMEM basic medium, and fetal bovine serum were purchased from Thermo Fisher Scientific (Shanghai, China). Bovine Serum Albumin (BSA) were purchased from Mao Kang Biotechnology (Shanghai, China). β-glycerophosphate, dexamethasone, and L-ascorbic acid were purchased from Sigma-Aldrich (Shanghai, China). Osteogenic-related primers (GAPDH, BMP-9, OCN, ALP) and immune-related primers (iNOS, TNF-α, Arg-1, CD206) were purchased from Sangon Biotech (Shanghai, China). Antimouse CD80 antibody and Antimouse CD206 antibody, were purchased from BioLegend (Beijing, China). RNA purification kits were purchased from Yisheng Biotechnology (Shanghai, China). Reverse transcription reaction kits were purchased from Novogene (Nanjing, China). Penicillin-streptomycin solution, alkaline phosphatase (ALP) staining kit, and Alizarin Red staining kit were purchased from Solarbio (Beijing, China). Lipopolysaccharide (LPS) and Cell Counting Kit-8 (CCK-8) were purchased from Beyotime Biotechnology (Shanghai, China). All other chemicals were purchased from Aladdin Reagent Co., Ltd. (Shanghai, China). All chemicals were used without further purification, and all experiments were performed using deionized water.

2.1. Cell Lines and Culture. MC3T3-E1 cells were cultured in α-MEM containing 10% fetal calf serum, 0.1 mg/mL streptomycin, and 100 U/mL penicillin. Cells were cultured at 37 °C and 5% CO_2. Mouse mononuclear macrophage leukemia cells (Raw 264.7) were cultured in high-glucose DMEM containing 10% fetal calf serum, 0.1 mg/mL streptomycin, and 100 U/mL penicillin. The osteogenesis induction medium was composed of 10% fetal bovine serum, 1% streptomycin, 1% penicillin, 10 mM β-glycerophosphate, 10 nM dexamethasone, and 50 μg/mL L-ascorbic acid.

2.2. Hydrogel Preparation. PVA and different proportions of Res were weighed and mixed, then combined with 25 mL of deionized water to adjust the PVA concentration to 10 wt % and the Res content to 0.4, 1.2, or 2.0%. The mixture was stirred further at 90 °C for 1 h to produce a uniformly dispersed solution. After removing bubbles with ultrasound, the mixture was poured into molds and allowed to cool to 25 °C, naturally forming a hydrogel. The resulting hydrogel was rapidly frozen at −80 °C for 12 h, then taken out and returned to 25 °C, resulting in PVA-Res hydrogels, labeled as 0.4, 1.2, and 2.0% respectively.

2.3. Extraction Solution Preparation. Each group of prepared hydrogel scaffolds was cut into samples measuring 1 mm thick, 1 × 1 cm, and weighing 0.1 g, and placed in culture dishes. The scaffolds were sterilized by UV irradiation for 2 h. After sterilization, the scaffolds were washed twice with phosphate-buffered saline (PBS) and soaked in serum-free α-MEM or DMEM at a ratio of 0.1 g/10 mL for 24 h. The resulting hydrogel extracts were stored at −20 °C for future use, and 10% serum and antibiotics were added to the hydrogel extracts for cell proliferation experiments. Serum and osteogenic induction factors were added to the extracts used in the ALP and alizarin red staining, as well as in the RT-qPCR experiments.

2.4. Characterization. The PVA and PVA−Res samples were vacuum-dried. The Fourier-transform infrared (FTIR) spectra of Res and freeze−thawed PVA and PVA−Res hydrogels were acquired at 500−4000 cm^{-1} by using an AVATAR 360 system (Nicolon Instruments, the USA) at 25 °C. Spectral analysis was performed on vacuum-dried PVA and PVA−Res samples at different concentrations. X-ray diffraction (XRD) studies were conducted by using an X-ray diffractometer (D8 Advance, Shanghai Zhujin Analytical Instrument Co., Ltd.) and Cu Kα radiation over the 2θ range of 5−60°. The crystallinity of the gel samples was evaluated as the ratio between the area of the crystalline reflection in the 2θ range 5−60° and the area subtending the whole diffraction profile of the gel sample. The morphological characteristics of the hydrogel surface were observed using scanning electron microscopy (SEM, SU-70, Hitachi, Japan).

https://doi.org/10.1021/acsomega.4c02849
ACS Omega 2024, 9, 49043−49053

Table 1. Sequences of Osteogenic Primers

gene	upstream sequence (5′−3′)	downstream sequence (5′−3′)
GAPDH	CACCACCAACTGCTTAGC	TTCACCACCTTCTTGATGTC
BMP-9	AGCTCCGACTCTATGTCTCCTG	CTGTCTTCACAAGCATGGTCTC
OCN	ACCATCTTTCTGCTCACTCTGCT	CCTTATTGCCCTCCTGCTTG
ALP	TTCAAACCGAGATACAAGCACT	GGGCCAGACCAAAGATAGAG

Table 2. Immune-associated Primer Sequences

gene	upstream sequence (5′−3′)	downstream sequence (5′−3′)
GAPDH	CACCACCAACTGCTTAGC	TTCACCACCTTCTTGATGTC
iNOS	ACTCAGCCAAGCCCTCACCTAC	TCCAATCTCTGCCTATCCGTCTCG
TNF-α	GCGACGTGGAACTGGCAGAAG	GCCACAAGCAGGAATGAGAAGAGG
Arg-1	AACCTTGGCTTGCTTCGGAACTC	GTTCTGTCTGCTTTGCTGTGATGC
CD206	AGGACGAAAGGCGGGATG	TTGGGTTCAGGAGTTGTTGTG

2.5. Rheology. The rheological behavior of hydrogels (20 mm diameter, 1 mm height) was analyzed by using a rotational rheometer (Kinexus Pro, Malvern Instruments). Temperature scan tests were performed at 25−80 °C and ω = 0.1 rad/s. Frequency (ω) sweep tests were performed at ω = 0.1−100 rad/s and 37 °C. Stress−strain tests were conducted at 37 °C and ω = 0.1−100 rad/s to observe the viscoelastic properties of hydrogels. Tests were performed at a strain (γ) of 0.5%.

2.6. Compression Mechanical Testing. The compressive moduli of hydrogels (15 mm diameter, 15 mm height) were analyzed by using a biomaterial mechanical−testing machine (Bose ELF3200) with a compression rate of 0.05 mm/s. The formula for engineering stress (σ) is $\sigma = F/S$, where S is the cross-sectional area of the specimen and F is the load. The engineering strain (ε) is the change in specimen height (h) relative to the initial height (h_0) and was calculated as $\varepsilon = (h_0 - h)/h_0 \times 100\%$.

2.7. Determination of Res Release from Hydrogel Scaffolds In Vitro. Different formulations of 0.1 g PVA-Res hydrogel were added to a 50 mL centrifuge tube containing 10 mL of PBS (0.01 M, pH 7.4) to study the release rate of PVA-Res. The mixture was then shaken at 37 °C and 70 rpm. At each time point (1, 6, 12, 24, 48, 72, 96, 120, 144, 168, 192, 216, and 240 h), 2 mL of supernatant was collected. The drug concentration in the release solution was measured at 306 nm using a UV spectrophotometer, and the cumulative drug release was calculated. The experiment was repeated three times, and the results were expressed as the average.

2.8. Cell Proliferation. MC3T3-E1 cells were seeded in a 96-well plate at a density of 5 × 10^3 cells/well and incubated with fresh medium at 37 °C in 5% CO_2 for 24 h. After allowing the cells to adhere to the plate walls, the original medium was removed. In the experimental group, 200 μL of extracts with different hydrogel ratios were added to each well, while the control group received 200 μL of fresh medium per well. After incubating for 24 and 48 h at 37 °C in 5% CO_2, 100 μL of 10% CCK-8 solution was added to each well. After an additional 2 h incubation, the supernatant was transferred to a new culture dish. The optical density was measured at 450 nm using a microplate reader. The results were expressed as the average of three experiments.

2.9. ALP and Alizarin Red Staining. ALP and Alizarin Red staining were used to study the effects of hydrogel scaffolds on MC3T3-E1 cell differentiation and mineralization. MC3T3-E1 cells were seeded in a 6-well plate at a density of 5 × 10^4 cells/well and incubated until the cell confluence reached approximately 80%, at which point the original medium was aspirated. The negative control (NC) group was cultured with normal α-MEM, the positive control (PC) group was cultured with α-MEM containing osteogenic induction medium, and the experimental group was added with 2 mL of PVA hydrogel extract or 0.4% PVA-Res hydrogel extract. The corresponding culture medium was replaced every 3 days. After 7 days of culture, cells were fixed with 4% paraformaldehyde (20 min), washed three times with PBS, and stained with an NBT/BCIP ALP kit. Cell staining was observed under a light microscope. Following the same culture method described above, after 14 days of culture, cells were fixed with 4% paraformaldehyde (20 min), washed with PBS three times, stained with 2% Alizarin Red solution (30 min), and washed with deionized water three times. Cells were observed and photographed with an optical microscope. ImageJ software was used for image processing and semi-quantitative analysis.

2.10. RT-qPCR of Osteogenesis-Related Genes. MC3T3-E1 cells were seeded in a 6-well plate at a density of 3 × 10^4 cells/well and incubated until the cell confluence reached approximately 80%. The original culture medium was aspirated away. The positive control (PC) group was cultured with α-MEM containing osteogenic induction medium, and the experimental group was added with 2 mL of PVA and 0.4% PVA−Res hydrogel extract. The culture medium was changed every 3 days. After 7 days of culture, total mRNA was extracted by using a Quick-RNA purification kit. Reverse transcription was performed with a HiScript II Q RT SuperMix kit following the manufacturer's instructions. Finally, an SYBR Green Master Mix kit and real-time PCR system were used to detect the mRNA expression levels of the osteogenesis-related genes BMP-9, osteocalcin (OCN), and ALP. The $2^{-\Delta\Delta Ct}$ method was used to analyze the expression of target genes. GAPDH served as the endogenous control. The average of three experiments was taken as the result. Primer sequences are shown in Table 1.

2.11. RT-qPCR Detection of Macrophage Polarity-Related Genes. Lipopolysaccharide (LPS) was used to induce Raw 264.7 macrophages toward M1 polarization, simulating early inflammatory responses. Raw 264.7 cells were seeded in a 6-well plate at a density of 5 × 10^4 cells/well, with three parallel controls established for each group. Cells were incubated for 24 h until they adhered to the walls of the plates. The original culture medium was aspirated, and Raw 264.7 cells were stimulated with DMEM containing 1 μg/mL LPS for 24 h. After stimulation, cells were rinsed with PBS

https://doi.org/10.1021/acsomega.4c02849
ACS Omega 2024, 9, 49043−49053

three times. The experimental and PC groups were cultured with 2 mL/well of DMEM extract or DMEM only, respectively. After 48 h of culture, total mRNA was extracted as described previously. The mRNA expression levels of genes related to M1 (TNF-α and iNOS) and M2 (Arg-1 and CD206) were detected. The $2^{-\Delta\Delta Ct}$ method was used to analyze the expression of target genes. The expression of GAPDH served as an endogenous control. The average of three experiments was taken as the result. Primer sequences are presented in Table 2.

2.12. Flow Cytometric Determination of Macrophage Polarity. Flow cytometry was used to detect the expression of M1-type markers (CD80) and M2-type markers (CD206) in macrophages in the presence of PVA−Res hydrogel scaffolds. A Raw 264.7 cell suspension was seeded into a six-well plate at 5×10^4 cells/mL, and three parallel controls were established per group. Cells were incubated for 24 h until they adhered to the wall. The original culture medium was aspirated, and the Raw 264.7 cells were stimulated with DMEM containing 1 μg/mL LPS for 24 h. After stimulation, cells were rinsed with PBS three times. The experimental and PC groups were cultured with 2 mL/well of DMEM extract or DMEM only, respectively. After 24 h of culture, the cells were rinsed three times with PBS and incubated with 3% BSA for 1 h. The cells were then washed three times with PBS and centrifuged at 1500 rpm for 3 min. Finally, the cells were rinsed three times with PBS and centrifuged at 1500 rpm for 3 min. Antibodies to CD80 and CD206 markers were then added to cells and stained for 40 min in the dark. The stained cells were diluted with 500 μL of cell-staining buffer, resuspended, and assessed via flow cytometry. Data were processed with FlowJo software.

2.13. Statistical Analysis. All quantitative data are presented as mean ± standard deviation. Statistical analysis was performed using one-way analysis of variance (ANOVA). Mean differences of $p < 0.05$ were considered statistically significant. Corresponding marks in figures are defined as $*p < 0.05$, $**p < 0.01$, $***p < 0.001$, $****P < 0.0001$.

3. RESULTS AND DISCUSSION

3.1. Preparation and Characterization of Hydrogels. The preparation and formation of PVA−Res hybrid hydrogels are shown in Figure 1. PVA solutions do not spontaneously form hydrogels at 25 °C or at high temperatures. Chen et al. used tannic acid as a cross-linking agent to improve the mechanical properties of PVA hydrogels; although the resulting hydrogel exhibited a tensile strength of 2.88 MPa and the elongation was increased by 1100%, the biological effect was poor.[32] In the current study, we mixed PVA with different concentrations of Res and stirred the mixtures at 90 °C for 2 h. After stirring, the 0.4% PVA−Res system appeared as a transparent liquid but turned milky white when cooled to 50 °C (Figure S1), whereas the 1.2 and 2.0% PVA-Res systems formed a milky-white mixed solution at 90 °C. When cooled to 25 °C, the 0.4, 1.2, and 2.0% PVA−Res systems all turned into milky-white solid gels with supportability and plasticity. The freeze−thaw method was then used to prepare the desired hydrogels, i.e., a sample was frozen at −80 °C for 12 h and thawed at 25 °C for 6 h to obtain the desired PVA−Res hydrogel. This approach shows that Res can be used as an efficient biological cross-linking agent for PVA hydrogels. The gelation of the PVA solution may be caused by the formation of strong hydrogen bonds between the hydrophobic drug Res and hydrophilic PVA via phenolic hydroxyl groups. Attenuated total reflection FTIR spectroscopy was performed on the Res, PVA, and PVA−Res hydrogels (Figure 2a). The FTIR spectrum of Res showed the characteristic stretching band of O−H at 3365 cm^{-1}, showing that the hydrogels were formed through the cross-linking of PVA and Res via hydrogen bonds. The FTIR spectrum of the PVA gel showed a characteristic stretching band of O−H at 3275 cm^{-1}, whereas in the FTIR spectrum of the PVA−Res hydrogel, this band shifted to 3268 cm^{-1}. The shift of the infrared absorption band to the low wavenumber indicates the formation of strong hydrogen bonds.

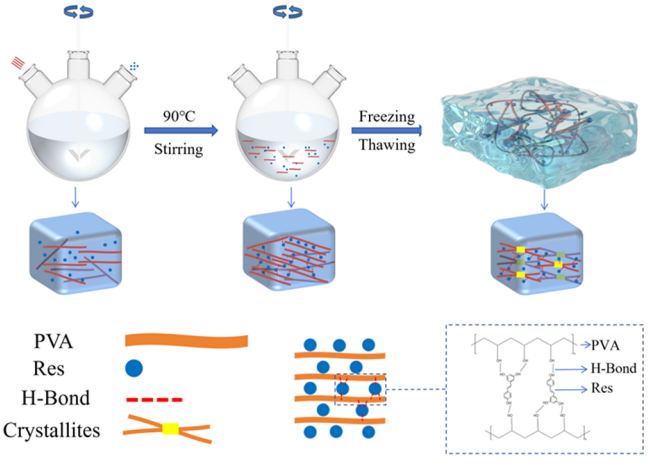

Figure 1. Preparation process of PVA−Res hydrogels.

The prepared samples were freeze-dried, crushed, and subjected to XRD (Figure 2b). Crystals were formed during lyophilization. The pure Res sample was a white powder, and the XRD pattern contained multiple typical peaks, indicating the presence of complex polymorphic features (Figure S2). The pure PVA gel exhibited sharp crystalline reflections, with a prominent peak at d = 4.50 Å (2θ = 19.7°), corresponding to the typical microcrystalline planes of irregular PVA. Additionally, two weak diffraction peaks were present at d = 3.83 Å (2θ = 23.2°) and d = 2.22 Å (2θ = 40.6°). Conversely, the 0.4, 1.2, and 2.0% PVA−Res gels had weak absorption peaks at 2θ = 19.6°. Moreover, as inferred from their XRD patterns, the pure PVA and 0.4, 1.2, and 2.0% PVA−Res hydrogels had crystallinities of 41, 27, 20, and 27%, respectively. Despite the increasing concentration of the cross-linking agent, the crystallinity of 2.0% PVA−Res was greater than that of 1.2% PVA−Res. This could be due to the gradual saturation of cross-linking between Res and PVA as the Res content increased. When the Res content exceeded 1.2 wt %, this surpassed its solubility in water, forming insoluble particles that hindered the cross-linking between Res and PVA and produced an unstable system. The 1.2% PVA−Res hydrogel had the lowest crystallinity among the gels, where hydrogen bonds between PVA and Res prevented the formation of PVA microcrystals.

SEM was used to observe the surfaces of the hydrogels to study their physical structure. Hydrogels typically contain a regular 3D framework and water, and hydrogen bonding may affect their structures. The pore structures in the frameworks were observed via SEM after the removal of water through freeze-drying. The PVA samples after freeze-drying exhibited large, porous, and irregularly arranged pore wall structures, whereas the 0.4% PVA−Res samples exhibited a relatively

https://doi.org/10.1021/acsomega.4c02849
ACS Omega 2024, 9, 49043−49053

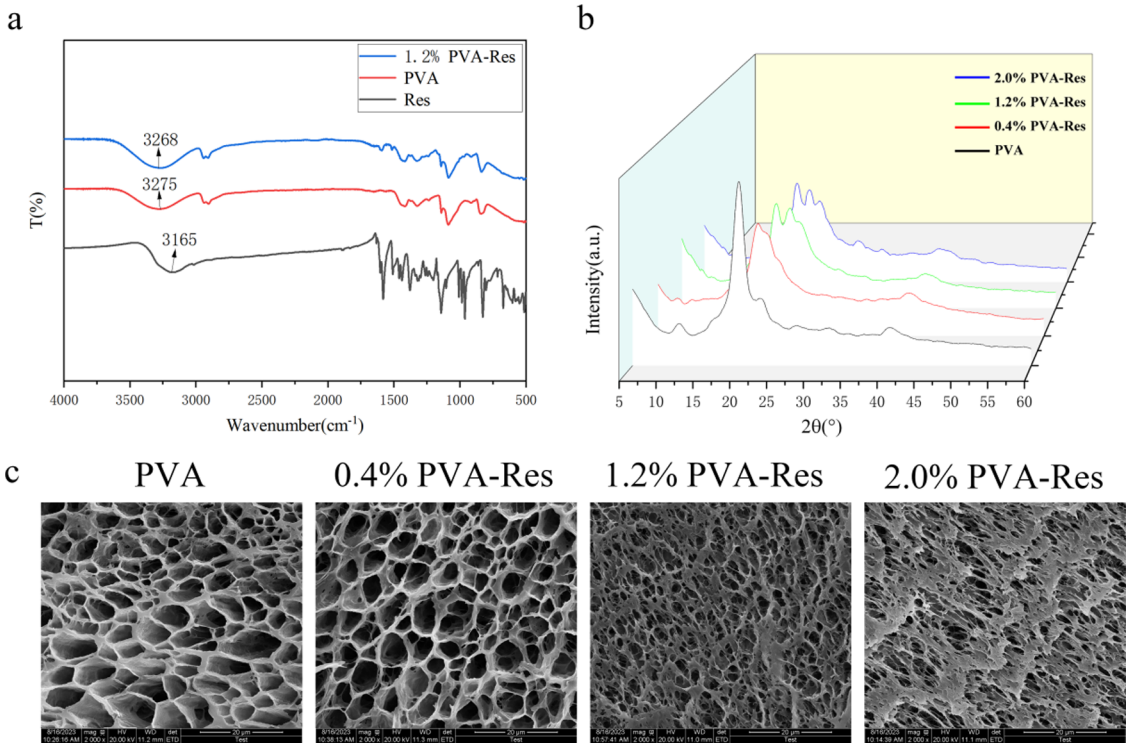

Figure 2. Characterization of different PVA−Res. (a) FTIR spectrum of PVA, Res, and 1.2% PVA−Res. (b) X-ray diffraction (XRD) patterns of PVA, 0.4% PVA−Res, 1.2% PVA−Res, and 2.0% PVA−Res. (c) SEM images of PVA, 0.4% PVA-Res, 1.2% PVA−Res, and 2.0% PVA−Res. Scale bar = 20 μm.

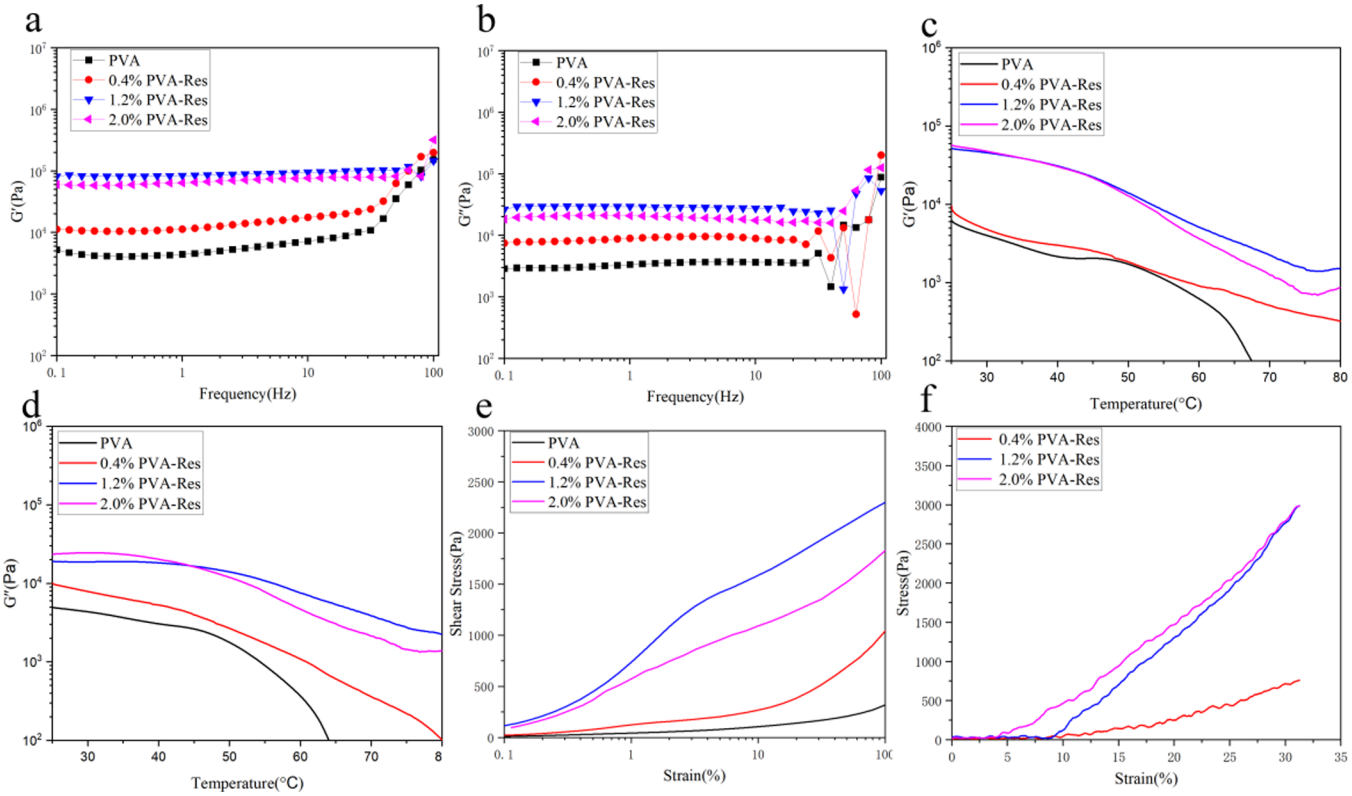

Figure 3. Rheological and compression properties of freeze−thawed hydrogels. (a) Frequency sweep test of PVA-Res G' values. (b) Frequency sweep test of PVA−Res G'' values. (c) Temperature sweep test of PVA−Res hydrogel G' values. (d) Temperature sweep test of PVA−Res hydrogel G'' values. (e) Stress−strain behavior curves. (f) Compression mechanical testing.

https://doi.org/10.1021/acsomega.4c02849
ACS Omega 2024, 9, 49043−49053

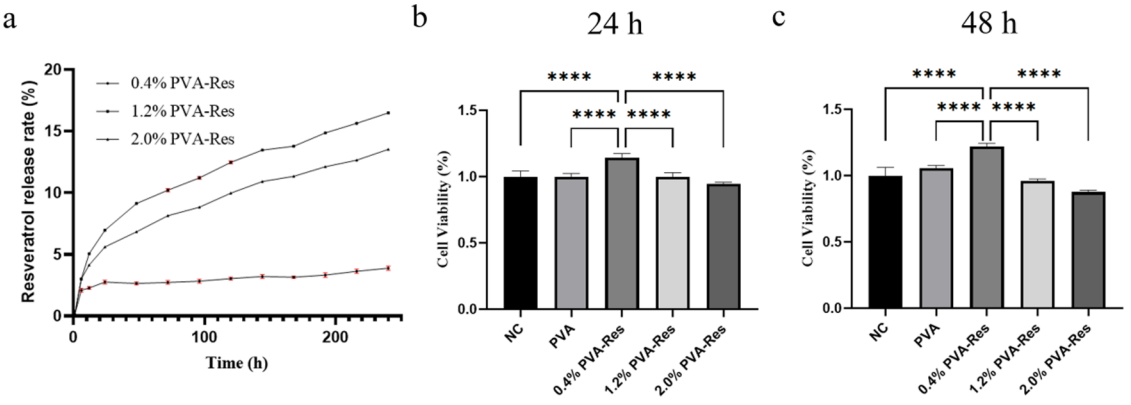

Figure 4. Drug release test and cell proliferation. (a) Resveratrol drug release of 0.4% PVA−Res hydrogels, 1.2% PVA−Res hydrogels, and 2.0% PVA−Res hydrogels within 240 h. (b) CCK-8 assay of MC3T3-E1 cell proliferation with different concentrations of extracts after 24 h. (c) CCK-8 assay of MC3T3-E1 cell proliferation with different concentrations of extracts after 48 h. *$p < 0.05$, **$p < 0.01$, ***$p < 0.001$, ****$p < 0.0001$.

uniform and regular arrangement of pores (Figure 2c). However, at concentrations above 0.4%, the PVA-Res group exhibited a loose and irregular pore wall structure, which may be due to the insoluble phase in the mixed solution.

3.2. Rheological and Compression Properties of Freeze−Thawed Hydrogels. The potential freeze−thaw preparation process based on the above results is shown in Figure 1. The PVA gel formed after treatment through the classic freeze−thaw method also considerably improved the stability of the PVA−Res hydrogels. The rheological properties of the PVA and PVA−Res hydrogels were studied through the frequency sweep method (0.1−100 Hz) to elucidate their stability. The PVA and PVA−Res hydrogels exhibited similar nonlinear rheological behaviors (Figure 3a,b), i.e., their storage modulus (G') and loss modulus (G'') changed with frequency and gradually increased with increasing frequency. At the same time and consistent with their solid-like state, their G' was higher than their G'' over the entire frequency range of 0.1−100 Hz, indicating that the 3D networks in their systems had good stability. The increase in the concentration of Res significantly increased the G' of the hydrogels, with the 1.2% PVA−Res hydrogel showing the maximal G' among the hydrogels. However, further increasing the Res concentration from 1.2 to 2.0% reduced G' and G''.

A rheometer was used to test the thermal stability of the PVA and 0.4, 1.2, and 2.0% PVA−Res hydrogels with increasing temperatures (25 to 80 °C) to determine the liquid and solid critical points of the hydrogels. Figure 3c,d shows the changes in the moduli of the PVA and Res−PVA hydrogels with increasing temperature and the gel−sol transition temperatures of the PVA and PVA−Res hydrogels as a function of Res concentration. The gel−sol transition temperature gradually increased with the increase in Res concentration. However, when the Res concentration exceeded 1.2%, the gel−sol transition temperature decreased. Thus, although Res can be used to effectively adjust the gel−sol transition temperature to increase the thermal stability of the hydrogels, this destroyed the cross-linking of the hydrogels above a certain concentration. The shear strains of the PVA and PVA−Res hydrogels are shown in Figure 3e. The viscoelastic modulus increased with the increase in Res concentration but decreased when the Res concentration exceeded 1.2%. The viscoelastic modulus of the 1.2% PVA−Res hydrogel increased by 8.5-fold relative to that of the PVA hydrogel. The 1.2% PVA−Res hydrogel also had good plasticity because of its temperature-responsive characteristics (Figure S3).

Notably, the pure PVA hydrogel lacked support ability at 25 °C, and the compression test was only performed using the hydrogels mixed with Res (Figure 3f). The results showed that Res improved the mechanical properties of the PVA hydrogels. The compressive modulus of the 1.2% PVA−Res hydrogel was 3.9-fold higher than that of the 0.4% PVA−Res gel. However, similar to previous results, increasing the Res concentration from 1.2 to 2.0% did not increase the compressive modulus of the gels. An excessive concentration of Res cannot improve the performance of the hydrogels and may reduce the stability of the hydrogels. In addition, the 1.2% PVA−Res hydrogel had good tensile properties, allowing a 3-fold length extension (Figure S4). The rheology experiment shows that the 1.2% PVA−Res hydrogel had excellent stability and mechanical properties.

3.3. Drug Release Assay. We conducted a drug release experiment on the 0.4% PVA−Res hydrogel, 1.2% PVA−Res hydrogel and 2.0% PVA−Res hydrogel. Res was continuously released for 240 h (approximately 10 days), and 0.4% PVA−Res hydrogel cumulative release amount reached 3.2% (Figure 4a). Increasing the number of days may increase the total amount of sustained drug release. Hydrophobic drugs may be trapped within the polymer network, slowing drug release.[33] In the first 24 h, Res only showed an initial burst release (2.7%), indicating that the release was controlled by a diffusion mechanism that was due to the physical interactions with PVA. In contrast, the 1.2% PVA−Res hydrogel group and the 2.0% PVA−Res hydrogel group exhibited rapid release within the first 24 h, with cumulative releases of 6.9 and 5.6%, respectively, during this period. Our experimental results indicate that compared to the 1.2% PVA−Res hydrogel group and the 2.0% PVA−Res hydrogel group, the 0.4% PVA−Res hydrogel can prolong drug release time and maintain an effective drug concentration for up to 240 h. The strong hydrogen bonds that formed between PVA and Res in the hydrogels may cause the release of some drug molecules, whereas the 3D network of the hydrogel limits this.[34] Drug release behavior is mainly due to the disruption of hydrogen bonds in the polymer, which causes the physical diffusion of Res.

3.4. Cell Proliferation Assay. The CCK-8 method was used to detect the proliferation of MC3T3-E1 cells cocultured with extracts of different concentrations of PVA−Res hydrogel

https://doi.org/10.1021/acsomega.4c02849
ACS Omega 2024, 9, 49043−49053

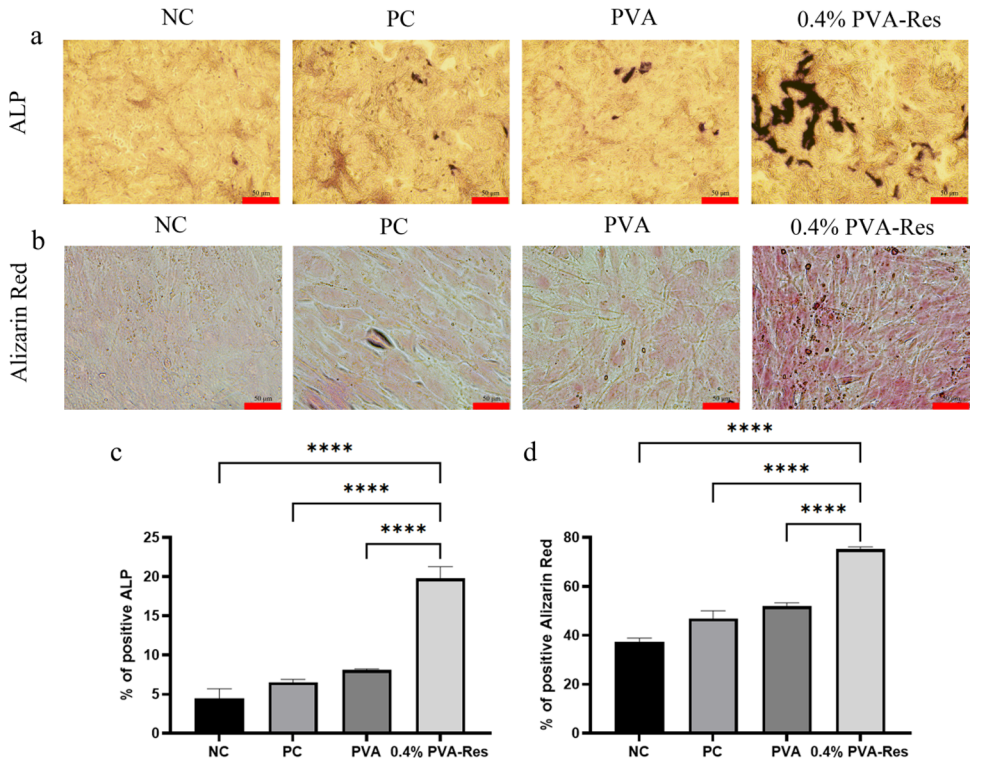

Figure 5. ALP and Alizarin Red staining experiment. (a) ALP staining of various group-stimulated cells for 7 days. (b) Alizarin red staining of various group-stimulated cells for 14 days. (c) Corresponding semiquantitative analysis of ALP results. (d) Semiquantitative analysis of Alizarin Red results (scale bar = 50 μm). *p < 0.05, **p < 0.01, ***p < 0.001, ****p < 0.0001.

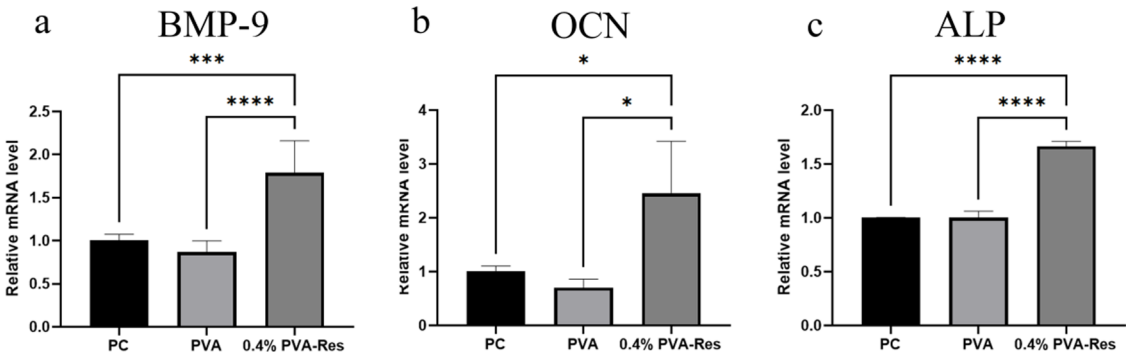

Figure 6. Detection of osteogenesis-related genes. (a−c) qPCR analysis of the osteogenesis-related gene expression of BMP-9, OCN, and ALP in MC3T3-E1 at day 7. *p < 0.05, **p < 0.01, ***p < 0.001, ****p < 0.0001.

for 24 and 48 h. No significant change in cell viability was found between the PVA hydrogel and control groups, suggesting that PVA hydrogel is noncytotoxic (Figure 4b,c); however, with the addition of Res, the 0.4% PVA−Res hydrogel supported higher cell viability at 24 and 48 h. When the Res content was >0.4 wt %, the cell viability noticeably decreased. This could be due to the increased release of Res with increasing cross-linking density, where higher concentrations of Res inhibited the growth of MC3T3-E1 cells. This finding is consistent with Cai,[35] who showed inhibition of cell proliferation and differentiation at Res concentrations above 100 μM. As the 0.4% PVA-Res hydrogel had the best effect of promoting cell proliferation (Figure 4b,c) and differentiation (Figure S5), we selected this hydrogel for subsequent experiments.

3.5. ALP and Alizarin Red Staining Experiment. Zhu et al. loaded Res on polycaprolactone (PCL)/chitosan (CS)/PVA-guided bone regeneration membranes, conferring the PCL/CS/PVA membranes with good osteogenic induction ability.[36] In the current study, we directly self-cross-linked Res and PVA to form hydrogels and performed ALP and Alizarin Red staining to evaluate the osteogenic potential of the PVA−Res hydrogels (Figure 5a,b). MC3T3-E1 cells were induced with hydrogel extract with added serum and osteogenic factors for 7 and 14 days and stained with ALP and Alizarin Red. Corresponding micrographs were taken and quantitatively analyzed. The 0.4% PVA−Res group showed the highest ALP and Alizarin Red activities among all groups, indicating that Res released from the 0.4% PVA−Res hydrogel had a bone-promoting effect (Figure 5c,d). Quantitative analysis revealed that after hydrogel treatment, the ALP-positive area in the 0.4% PVA−Res group was 4.4-, 3-, and 2.4-fold that in the NC, PC, and PVA groups. The positive area of Alizarin Red in the 0.4% PVA−Res group was 2-, 1.6-, and 1.4-fold that in the NC,

https://doi.org/10.1021/acsomega.4c02849
ACS Omega 2024, 9, 49043−49053

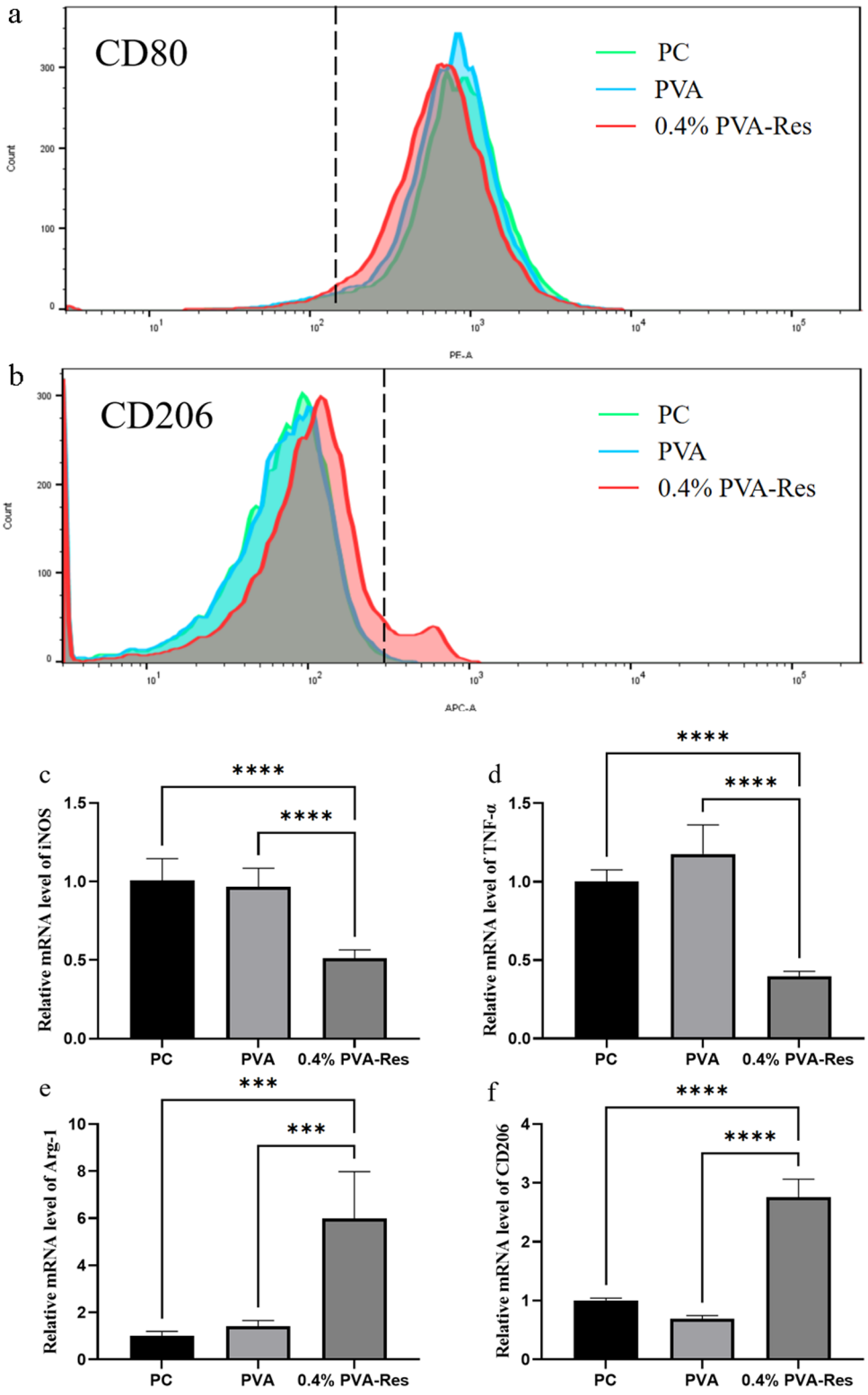

Figure 7. Flow cytometry for the determination and detection of macrophage polarity and immune-related genes. (a, b) CD80-positive cells and CD206-positive cells were detected by flow cytometry. (c–f) Evaluation of the immunomodulatory effects of the PVA–Res hydrogel with Raw 264.7 cells after 24 h culture: M1-related (iNOS and TNF-α) and M2-related (Arg-1 and CD206) mRNA expressions. *$p < 0.05$, **$p < 0.01$, ***$p < 0.001$, ****$p < 0.0001$.

PC, and PVA groups. The above results confirm that the 0.4% PVA–Res hydrogel has good bone-promoting properties.

3.6. Expression of Osteogenesis-Related Genes. Cells were cultured in the osteogenic induction medium with added hydrogel extract for 7 days, and the expression of osteogenesis-related genes was detected via qPCR to study the effect of the 0.4% PVA–Res hydrogel on the osteogenic differentiation of MC3T3-E1 cells. The expression levels of the osteogenic BMP-9, OCN, and ALP genes in the 0.4% PVA–Res group were 2.1-, 3.5-, and 1.7-fold those in the PVA group,

https://doi.org/10.1021/acsomega.4c02849
ACS Omega 2024, 9, 49043–49053

respectively (Figure 6a−c). Wang et al. identified that Res can not only enhance osteogenic induction alone but can also be used in combination with BMP-9, producing significant increases in the expression of early osteogenic markers (ALP, Runx2, and SP7) as well as that of late osteogenic markers (OPN and OCN).[37] These results suggest that the 0.4% PVA-Res hydrogel may promote the expression of osteogenic genes in osteogenic induction culture.

3.7. Flow Cytometric Determination and Detection of Macrophage Polarity and Immune-Related Genes. Res can alleviate the expression of proinflammatory factors (iNOS, COX-2, and NO).[38] We investigated the immunomodulatory effects of hydrogels on macrophages using flow cytometry. As shown in Figure 7a, CD80-positive cells treated with 0.4% PVA−Res hydrogel exhibited a slight downregulation compared to the PC and PVA groups. In Figure 7b, the expression of CD206-positive cells treated with 0.4% PVA−Res hydrogel was significantly increased. This suggests that the 0.4% PVA−Res hydrogel may induce polarization of Raw264.7 cells toward the M2 phenotype and potentially promote the transition of M1-type Raw264.7 cells to the M2 type.

Res suppresses inflammation by inhibiting the activation of the NF-κB-signaling pathway.[39] Raw 264.7 expresses Arg-1 and CD206 through the activation of the STAT3 pathway.[40] The effect of Res-containing PVA hydrogels on macrophage polarization was further examined through qPCR. The expression of genes encoding inflammatory markers (iNOS and TNF-α) in the 0.4% PVA−Res group was significantly downregulated relative to that in the PC group (Figure 7c,d). The iNOS and TNF-α mRNA expression levels in the 0.4% PVA−Res hydrogel group were downregulated by 0.66- and 0.62-fold relative to those in the PC group. However, no significant difference was found between the PVA hydrogel and PC groups. Conversely, the expression of M2-related genes (Arg-1, CD206) was significantly upregulated in cells treated with the extract (Figure 7e,f). The mRNA expression levels of Arg-1 and CD206 in the 0.4% PVA−Res hydrogel group were 5.9- and 1.7-fold higher than those in the PC group, respectively. Wang et al. found that in SNI rats, Res can inhibit microglion-mediated neuroinflammation by regulating the TREM2−autophagy axis. They showed that Res can downregulate TNF-α, IL-6, and IL-1β expression levels,[41] which is similar to our results. Our results indicate that Res can effectively act on macrophages, promoting the M2 differentiation of Raw 264.7 cells by regulating the immune microenvironment and inhibiting the expression of proinflammatory mediators.

4. CONCLUSIONS

PVA and Res hydrogels with different proportions (0.4, 1.2, and 2.0% PVA−Res) were prepared through mixing, heating, freezing, and dissolution. The PVA−Res hydrogels were prepared through a simple and green preparation process and had favorable stability and mechanical properties. The viscoelastic modulus of the 1.2% PVA−Res hydrogel was 8.5-fold higher than that of the pure PVA hydrogel. The 0.4% PVA−Res hydrogel promoted osteoblast proliferation and cell osteogenic differentiation and had good mineralization effects. The 0.4% PVA-Res hydrogel extract enhanced the expression of osteogenic genes BMP-9, cyanate, and ALP in MC3T3-E1 cells, significantly downregulated the mRNA expression of M1-related genes (iNOS and TNF-α) in LPS-activated Raw 264.7 cells, and promoted the mRNA expression of M2-related genes (Arg-1 and CD206). Therefore, PVA-Res hydrogel materials hold promise for applications in the field of bone injury repair.

■ ASSOCIATED CONTENT

Data Availability Statement

All available data can be found within the article and in the supplementary file. Further inquiries can be directed to the corresponding author.

Supporting Information

The Supporting Information is available free of charge at https://pubs.acs.org/doi/10.1021/acsomega.4c02849.

Effect of temperature on 0.4% PVA-Res hydrogel (Figure S1); X-ray diffraction pattern of Res (Figure S2); plasticity of 1.2% PVA-Res hydrogel (Figure S3); tensile properties of 1.2% PVA-Res hydrogel (Figure S4); and ALP staining of various groups-stimulated cells for 7 days (Figure S5) (PDF)

■ AUTHOR INFORMATION

Corresponding Authors

Xinye Ni − *Department of Radiotherapy Oncology, Changzhou No.2 People's Hospital, Nanjing Medical University, Changzhou 213003, China; Jiangsu Province Engineering Research Center of Medical Physics, Changzhou 213003, China; Changzhou Key Laboratory of Medical Physics, Changzhou 213003, China;* orcid.org/0000-0002-2402-9719; Email: nxy@njmu.edu.cn

Cheli Wang − *School of Pharmacy, Changzhou University, Changzhou 213000, China*; Email: clwang@cczu.edu.cn

Authors

Pengyin Li − *School of Pharmacy, Changzhou University, Changzhou 213000, China; Department of Radiotherapy Oncology, Changzhou No.2 People's Hospital, Nanjing Medical University, Changzhou 213003, China; Jiangsu Province Engineering Research Center of Medical Physics, Changzhou 213003, China; Changzhou Key Laboratory of Medical Physics, Changzhou 213003, China*

Shaoqing Chen − *Department of Radiotherapy Oncology, Changzhou No.2 People's Hospital, Nanjing Medical University, Changzhou 213003, China; Jiangsu Province Engineering Research Center of Medical Physics, Changzhou 213003, China; Changzhou Key Laboratory of Medical Physics, Changzhou 213003, China*

Yanyan Meng − *School of Pharmacy, Changzhou University, Changzhou 213000, China; Department of Radiotherapy Oncology, Changzhou No.2 People's Hospital, Nanjing Medical University, Changzhou 213003, China; Jiangsu Province Engineering Research Center of Medical Physics, Changzhou 213003, China; Changzhou Key Laboratory of Medical Physics, Changzhou 213003, China*

Complete contact information is available at: https://pubs.acs.org/10.1021/acsomega.4c02849

Author Contributions

P.L.: Conceptualization, methodology, data curation, funding acquisition, and writing—original draft preparation. S.C.: Methodology, data curation, and formal analysis. Y.M.: Visualization, investigation, data curation, and resources. C.W.: Conceptualization, writing—reviewing and editing. X.N.: Conceptualization, funding acquisition, writing—review-

https://doi.org/10.1021/acsomega.4c02849
ACS Omega 2024, 9, 49043−49053

ing and editing. P.L. and S.C. have contributed equally to this work.

Notes

The authors declare no competing financial interest.

■ ACKNOWLEDGMENTS

The author(s) disclosed receipt of the following financial support for the research, authorship, and/or publication of this: This work has been supported by the National Natural Science Foundation of China under Grant No.81871756 and Innovation Fund of National Orthopedics and Exercise Rehabilitation Clinical Medical Research Center (research number: 2021-NCRC-CXJJ-ZH-13).

■ REFERENCES

(1) Wu, Y.; Li, X.; Wang, Y.; et al. Research progress on mechanical properties and wear resistance of cartilage repair hydrogel. *Materials & Design* **2022**, *216*, No. 110575.
(2) Liu, M.; Zeng, X.; Ma, C.; et al. Injectable hydrogels for cartilage and bone tissue engineering. *Bone Res.* **2017**, *5* (1), 17014.
(3) Yue, S.; He, H.; Li, B.; et al. Hydrogel as a biomaterial for bone tissue engineering: A review. *Nanomaterials* **2020**, *10* (8), 1511.
(4) Burger, D.; Beaumont, M.; Rosenau, T.; et al. Porous silk fibroin/cellulose hydrogels for bone tissue engineering via a novel combined process based on sequential regeneration and porogen leaching. *Molecules* **2020**, *25* (21), 5097.
(5) Aslam, M.; Kalyar, M. A.; Raza, Z. A. Polyvinyl alcohol: A review of research status and use of polyvinyl alcohol based nanocomposites. *Polym. Eng. Sci.* **2018**, *58* (12), 2119−2132.
(6) Wang, M.; Bai, J.; Shao, K.; et al. Poly (vinyl alcohol) hydrogels: The old and new functional materials. *International Journal of Polymer Science* **2021**, *2021*, 1−16.
(7) Mandru, M.; Bercea, M.; Gradinaru, L. M.; et al. Polyurethane/poly (vinyl alcohol) hydrogels: Preparation, characterization and drug delivery. *Eur. Polym. J.* **2019**, *118*, 137−145.
(8) Han, Y.; Li, C.; Cai, Q.; et al. Studies on bacterial cellulose/poly (vinyl alcohol) hydrogel composites as tissue-engineered corneal stroma. *Biomedical Materials* **2020**, *15* (3), No. 035022.
(9) Tang, Z.; Yu, M.; Mondal, A. K.; et al. Porous Scaffolds Based on Polydopamine/Chondroitin Sulfate/Polyvinyl Alcohol Composite Hydrogels. *Polymers* **2023**, *15* (2), 271.
(10) Munir, M. U.; Mikucioniene, D.; Khanzada, H.; et al. Development of eco-friendly nanomembranes of aloe vera/PVA/ZnO for potential applications in medical devices. *Polymers* **2022**, *14* (5), 1029.
(11) Xu, M.; Qin, M.; Zhang, X.; et al. Porous PVA/SA/HA hydrogels fabricated by dual-crosslinking method for bone tissue engineering. *Journal of Biomaterials Science, Polymer Edition* **2020**, *31* (6), 816−831.
(12) Li, F.; Wang, A.; Wang, C. Analysis of friction between articular cartilage and polyvinyl alcohol hydrogel artificial cartilage. *J. Mater. Sci.: Mater. Med.* **2016**, *27*, 87.
(13) Liu, T.; Peng, X.; Chen, Y. N.; et al. Hydrogen-bonded polymer−small molecule complexes with tunable mechanical properties. *Macromol. Rapid Commun.* **2018**, *39* (9), No. 1800050.
(14) Zuluaga, M.; Gregnanin, G.; Cencetti, C.; et al. PVA/Dextran hydrogel patches as delivery system of antioxidant astaxanthin: A cardiovascular approach. *Biomedical Materials* **2018**, *13* (1), No. 015020.
(15) Bercea, M.; Biliuta, G.; Avadanei, M.; et al. Self-healing hydrogels of oxidized pullulan and poly (vinyl alcohol). *Carbohydr. Polym.* **2019**, *206*, 210−219.
(16) Promdontree, P.; Kheolamai, P.; Ounkaew, A.; et al. Characterization of Cellulose Fiber Derived from Hemp and Polyvinyl Alcohol-Based Composite Hydrogel as a Scaffold Material. *Polymers* **2023**, *15* (20), 4098.
(17) Li, J.; Cao, X.; Liu, Y.; et al. Thermorheological complexity of poly (vinyl alcohol)/borax aqueous solutions. *J. Rheol.* **2020**, *64* (4), 991−1002.
(18) Kumar, G. C. M.; Jeyaraj, P.; Nagamadhu, M. Influence of glutaraldehyde on dynamic properties of poly (vinyl alcohol) polymer. *Emerg. Mater. Res.* **2020**, *9* (1), 168−179.
(19) Al-Sabagh, A. M.; Abdeen, Z. Preparation and characterization of hydrogel based on poly (vinyl alcohol) cross-linked by different cross-linkers used to dry organic solvents. *Journal of Polymers and the Environment* **2010**, *18*, 576−583.
(20) Zheng, J.; Fan, R.; Wu, H.; et al. Directed self-assembly of herbal small molecules into sustained release hydrogels for treating neural inflammation. *Nat. Commun.* **2019**, *10* (1), 1604.
(21) Song, X.; He, T.; Qi, Y.; et al. Properties of cell-compatible poly (vinyl alcohol) hydrogels cross-linked with hydrophobic luteolin. *ACS Applied Polymer Materials* **2021**, *3* (6), 3019−3027.
(22) Song, X.; Zhang, Z.; Shen, Z.; et al. Facile preparation of drug-releasing supramolecular hydrogel for preventing postoperative peritoneal adhesion. *ACS Appl. Mater. Interfaces* **2021**, *13* (48), 56881−56891.
(23) Wang, B.; Jiang, H. M.; Qi, L. M.; et al. Deciphering resveratrol's role in modulating pathological pain: From molecular mechanisms to clinical relevance. *Phytother. Res.* **2023**, *38*, 59−73.
(24) Marchal, J.; Pifferi, F.; Aujard, F. Resveratrol in mammals: effects on aging biomarkers, age-related diseases, and life span. *Ann. N.Y. Acad. Sci.* **2013**, *1290* (1), 67−73.
(25) Su, M.; Zhao, W.; Xu, S.; et al. Resveratrol in treating diabetes and its cardiovascular complications: a review of its mechanisms of action. *Antioxidants* **2022**, *11* (6), 1085.
(26) Chen, X.; Song, X.; Zhao, X.; et al. Insights into the Anti-inflammatory and Antiviral Mechanisms of Resveratrol. *Mediators Inflamm.* **2022**, *2022*, No. 7138756.
(27) Min, K. K.; Neupane, S.; Adhikari, N.; et al. Effects of resveratrol on bone-healing capacity in the mouse tooth extraction socket. *Journal of Periodontal Research* **2020**, *55* (2), 247−257.
(28) Duan, W. J.; Li, Y. F.; Liu, F. L.; et al. A SIRT3/AMPK/autophagy network orchestrates the protective effects of trans-resveratrol in stressed peritoneal macrophages and RAW 264.7 macrophages. *Free Radical Biol. Med.* **2016**, *95*, 230−242.
(29) Yuan, J.; et al. Resveratrol rescues TNF-α-induced inhibition of osteogenesis in human periodontal ligament stem cells via the ERK1/2 pathway. *Mol. Med. Rep.* **2020**, *21* (5), 2085−2094.
(30) Inchingolo, A. D.; Inchingolo, A. M.; Malcangi, G.; et al. Effects of Resveratrol, Curcumin and Quercetin Supplementation on Bone Metabolism—A Systematic Review. *Nutrients* **2022**, *14* (17), 3519.
(31) Li, L.; Yu, M.; Li, Y.; et al. Synergistic anti-inflammatory and osteogenic n-HA/resveratrol/chitosan composite microspheres for osteoporotic bone regeneration. *Bioactive materials* **2021**, *6* (5), 1255−1266.
(32) Chen, W.; Li, N.; Ma, Y.; et al. Superstrong and tough hydrogel through physical cross-linking and molecular alignment. *Biomacromolecules* **2019**, *20* (12), 4476−4484.
(33) Xu, J.; Wang, H.; Jiang, L.; et al. Preparation of cellulose hydrogel dressing with evenly dispersed hydrophobic drugs by hydrogen bonding and encapsulation methods. *Macromol. Mater. Eng.* **2021**, *306* (10), No. 2100286.
(34) Baksi, A.; Biswas, R. Does Confinement Modify Preferential Solvation and H-Bond Fluctuation Dynamics? A Molecular Level Investigation through Simulations of a Bulk and Confined Three-Component Mixture. *J. Phys. Chem. B* **2020**, *124* (51), 11718−11729.
(35) Cai, W.; Sun, B.; Song, C.; et al. Resveratrol induces proliferation and differentiation of mouse pre-osteoblast MC3T3-E1 by promoting autophagy. *BMC Complement. Med. Ther.* **2023**, *23* (1), 121.
(36) Zhu, Y.; Jiang, S.; Xu, D.; et al. Resveratrol-loaded co-axial electrospun poly (ε-caprolactone)/chitosan/polyvinyl alcohol membranes for promotion of cells osteogenesis and bone regeneration. *Int. J. Biol. Macromol.* **2023**, *249*, No. 126085.

https://doi.org/10.1021/acsomega.4c02849
ACS Omega 2024, 9, 49043−49053

(37) Wang, Y.; Xia, C.; Chen, Y.; et al. Resveratrol synergistically promotes BMP9-induced osteogenic differentiation of mesenchymal stem cells. *Stem Cells Int.* **2022**, *2022*, No. 8124085.
(38) Hsu, H. T.; Tseng, Y. T.; Wong, W. J.; et al. Resveratrol prevents nanoparticles-induced inflammation and oxidative stress via downregulation of PKC-α and NADPH oxidase in lung epithelial A549 cells. *BMC Complement. Altern. Med.* **2018**, *18* (1), 211.
(39) Yang, R.; Yan, Y.; Wu, Z.; et al. Resveratrol-loaded titania nanotube coatings promote osteogenesis and inhibit inflammation through reducing the reactive oxygen species production via regulation of NF-κB signaling pathway. *Materials Science and Engineering: C* **2021**, *131*, No. 112513.
(40) Liu, F. J.; Gu, T. J.; Wei, D. Y. Emodin alleviates sepsis-mediated lung injury via inhibition and reduction of NF-kB and HMGB1 pathways mediated by SIRT1. *Kaohsiung Journal of Medical Sciences* **2022**, *38* (3), 253−260.
(41) Wang, Y.; Shi, Y.; Huang, Y.; et al. Resveratrol mediates mechanical allodynia through modulating inflammatory response via the TREM2-autophagy axis in SNI rat model. *J. Neuroinflammation* **2020**, *17* (1), 311.

https://doi.org/10.1021/acsomega.4c02849
ACS Omega 2024, 9, 49043−49053